On the potential of transcutaneous auricular vagus nerve stimulation to reduce visually induced motion sickness

Emmanuel Molefi (em576@kent.ac.uk)
University of Kent
Ian McLoughlin
Singapore Institute of Technology
Ramaswamy Palaniappan
University of Kent

Article

Keywords:

Posted Date: September 9th, 2022

DOI: https://doi.org/10.21203/rs.3.rs-2039235/v1

On the potential of transcutaneous auricular vagus nerve stimulation to reduce visually induced motion sickness

Emmanuel Molefi[1,*], Ian McLoughlin[2], and Ramaswamy Palaniappan[1]

[1]Data Science Research Group, School of Computing, University of Kent, Canterbury, UK
[2]ICT Cluster, Singapore Institute of Technology, Singapore
[*]em576@kent.ac.uk

ABSTRACT

Transcutaneous auricular vagus nerve stimulation (taVNS) is a potent therapeutic tool for a broad spectrum of diseases and disorders. Here, we investigated the effects of taVNS on autonomic function during visually induced motion sickness, through the analysis of spectral and time-frequency heart rate variability. To determine the efficacy of taVNS, we compared sham and taVNS condition in a randomized, within-subjects, cross-over design in 14 healthy participants. We found that taVNS reduced motion sickness symptoms by significantly increasing normalized high-frequency (HF) power and decreasing both normalized low-frequency (LF) power and the power ratio of LF and HF components (sympathovagal balance). Furthermore, behavioral data recorded using the motion sickness assessment questionnaire (MSAQ) showed significant differences in decreased symptoms during taVNS compared to sham condition for the total MSAQ scores and, central and sopite categories of the MSAQ. Our findings suggest that by administering taVNS, parasympathetic modulation is increased, and autonomic imbalance induced by motion sickness is restored. This study provides first evidence that taVNS has potential as a non-pharmacological neuromodulation tool to keep motion sickness at bay. Thus, this sheds new light towards protecting people from becoming motion sick and possible accelerated recovery from the malady.

Introduction

Transcutaneous auricular vagus nerve stimulation (taVNS) is a neuromodulation technique for vagal afferent stimulation. Using skin electrodes, taVNS is administered non-invasively at the outer ear to target the auricular branch of the vagus nerve. From previous studies on taVNS, researchers have shown that by non-invasively stimulating these afferent fibres of the vagus nerve, positive therapeutic effects are elicited, for instance, in pharmacoresistant epilepsy[1], depression[2] and chronic migraine[3]. Another non-invasive approach is to stimulate the vagus nerve in the neck area, in a modality known as transcutaneous cervical vagus nerve stimulation (tcVNS). In fact, a recent study found that attaching surface electrodes to the neck, targeting the cervical branch of the vagus nerve, improved gait and motor function in Parkinson's disease patients[4].

The vagus nerve (cranial nerve X) originates from the brainstem in an area called the medulla oblongata. From there it extends bilaterally carrying parasympathetic innervation to the auricular branch, before travelling down the neck, targeting major organs in the thorax, and making its way down to the gastrointestinal tract. It forms a complex neural network comprising of afferent and efferent neural pathways. Essentially, the vagus nerve has crucial involvement on functions such as the autonomic, cardiovascular, respiratory, gastrointestinal, immune and endocrine systems[5]. From a neurophysiological viewpoint, it means we could stimulate the vagus nerve to interfere with motion sickness pathogenesis, aiming to restore autonomic imbalance. This segues us into motion sickness and its implications on modulating the autonomic nervous system (ANS). Together, the evidence prompts us to explore stimulating the vagus nerve to discern any impact on ameliorating symptoms of motion sickness.

Motion sickness is an age-old physiological malady associated with epigastric discomfort, nausea and, in its severity, emesis. More than 2000 years ago, the Greek physician Hippocrates observed this physiological phenomenon[6]. Alas, motion sickness still poses as an aversive experience in modern transportation. Although being a technological advancement for humanity, the advent of autonomous and semiautonomous vehicles may well heighten the incidence and risk of motion sickness[7,8]. Moreover, digital devices and displays also pose an emerging hazard to many prone to the ailment[9]. 3D displays have also been found to evoke symptoms of motion sickness in contrast to their 2D counterparts[10]. Not only is the quality of travel being affected by motion sickness, but also the quality of life.

Explanation for the aetiology of motion sickness is not well understood. Hence many theories aiming to elucidate its mechanisms have been proposed[8]. Currently, a widely influential theory is one proposed by Reason and Brand[6], defined as the

sensory conflict theory. This theory posits that because of ambiguous sensory information from the eyes and the vestibular system, motion sickness is onset. Reason[11] further developed the neural mismatch theory as a corollary to the sensory conflict theory. The symptomatology of motion sickness is characterised by a vast array of features which include, for instance, sweating, dizziness, drowsiness, headache, eyestrain, nausea and vomiting.

Motion sickness changes ANS response. Researchers have assessed this cardio-autonomic modulation by measuring electrocardiogram (ECG) signals and consequently deriving heart rate variability (HRV). Reported findings on decreased high frequency power (HF; 0.15-0.40 Hz) of the HRV spectra have been consistent[12–14]. Furthermore, multiple studies have shown that the power ratio between low frequency (LF; 0.04-0.15 Hz) and HF band powers (LF/HF) increases with symptom development of motion sickness[13,15,16]. Given that the aforementioned metrics are features of altered physiological arousal by motion sickness, which has no cure, studying these changes in ANS response could enable researchers to manipulate them for non-pharmacologic interventions including taVNS, in an effort to mitigate motion sickness. Sawada, *et al.*[17] show that visually induced motion sickness from driving simulators can be reduced by, for example, coupling presentation of sound and vibration. A recent report investigated the protective effects of transcutaneous electrical acustimulation (TEA) on motion sickness induced by a rotary chair[18]. Here, we propose a non-invasive taVNS neuromodulation application to help in the management of motion sickness.

Our primary hypothesis is that by administering taVNS simultaneously with increasing levels of motion sickness, the metrics for LF and LF/HF ratio would decrease while the HF metric would increase. Furthermore, we hypothesized that the aforementioned objective measurements would be complemented by decreases in the scores of behavioral measurements obtained using an established and validated tool, the motion sickness assessment questionnaire (MSAQ). This is capable of measuring the severity of motion sickness in four dimensions (gastrointestinal, central, peripheral, sopite). Our rationale on the potential therapeutic/interventional effects of taVNS being that by stimulating the vagus nerve, vagal tone would be potentiated and, thus, a restoration in the sympathovagal balance observed.

Results

We first sought to establish that the nauseogenic stimulation was inducing motion sickness by evaluating the HRV spectral parameters. Thus, baseline measurements were compared with "Nausea" measurements in the sham condition with the expectation that the parasympathetic tone would be decreased from baseline. Additionally, we expected the sympathovagal balance as measured by LF/HF ratio to increase from baseline.

As expected, we did find a significant decrease in parasympathetic activity measured by HF n.u. ($t_{(13)} = 3.29$, $p = 0.0029$) and increase in LF/HF ratio ($t_{(13)} = -3.39$, $p = 0.0024$) as shown in (Fig. 1a). This is in line with previous studies that found decreases and increases in normalized HF and LF/HF ratio respectively with increasing symptoms of motion sickness. Further, a significant increase from baseline during nausea was found for LF n.u. ($t_{(13)} = -3.27$, $p = 0.0030$). This result indicates that the nauseogenic stimulus was efficacious in eliciting robust physiological arousal.

The delta change of LF n.u. power and LF/HF ratio during nausea section and baseline was compared between sham and taVNS conditions (Fig. 1b). A significant decrease was found in LF n.u. ($t_{(13)} = 2.21$, $p = 0.0227$) and LF/HF ratio ($t_{(13)} = 2.37$, $p = 0.0170$) suggesting that taVNS was able to pull the level of autonomic arousal down. There was a significant increase in HF n.u. ($t_{(13)} = -2.23$, $p = 0.0220$) between sham and taVNS (Fig. 1b), indicating that taVNS was triggering an enhancement in vagal modulation.

The time-frequency representations of HRV were computed by performing smoothed pseudo Wigner-Ville distribution (SPWVD) for the sham and taVNS condition, and the difference between the two conditions (Fig. 2). SPWVD was used due to its ability to represent a signal in a robust manner in both time and frequency planes, circumventing trade-offs between time and frequency resolution. It also reveals dynamics of autonomic function during symptomatology development that may be associated with this complex syndrome. The blue colour in the time-frequency power map in (Fig. 2a) indicates that Baseline had higher power in those particular regions whereas it had lower power in the bright yellow regions. This also applies to the other time-frequency maps in (Fig. 2). Note that (Sham vs Baseline) is interpreted as performing the operation (Sham - Baseline), similarly to other time-frequency maps shown in (Fig. 2). We observe that in (Fig. 2a; Sham vs Baseline), the participant was showing attenuated HF power and increases in LF power for particular timepoints. While during (taVNS vs Baseline) the participant had a pronounced HF power at particular timepoints. The power difference between (taVNS vs Baseline) and (Sham vs Baseline) is shown in the bottom panel (Fig. 2a). We performed cluster-based permutation tests at the sample level. The power differences at the sample level are shown in (Fig. 2b; taVNS vs Sham). The resulting z-statistic map of (taVNS vs Sham) is shown in (Fig. 2c) with significant clusters shown in black contours. During taVNS stimulation, activity of HF HRV was increased (Fig. 2b); a cluster-based permutation test found 3 interpretable temporal clusters (cluster around 35-67 s, $z = 2.20$, $p = 0.0137$) and the other 2 clusters (at around 10 s) both significant at ($p_{corrected} < 0.0176$).

The MSAQ scores were computed as delta change from baseline then compared between sham and taVNS conditions (Fig. 3). In addition to Shapiro-Wilk normality test, histogram and normal probability visualisations were used as further tools to

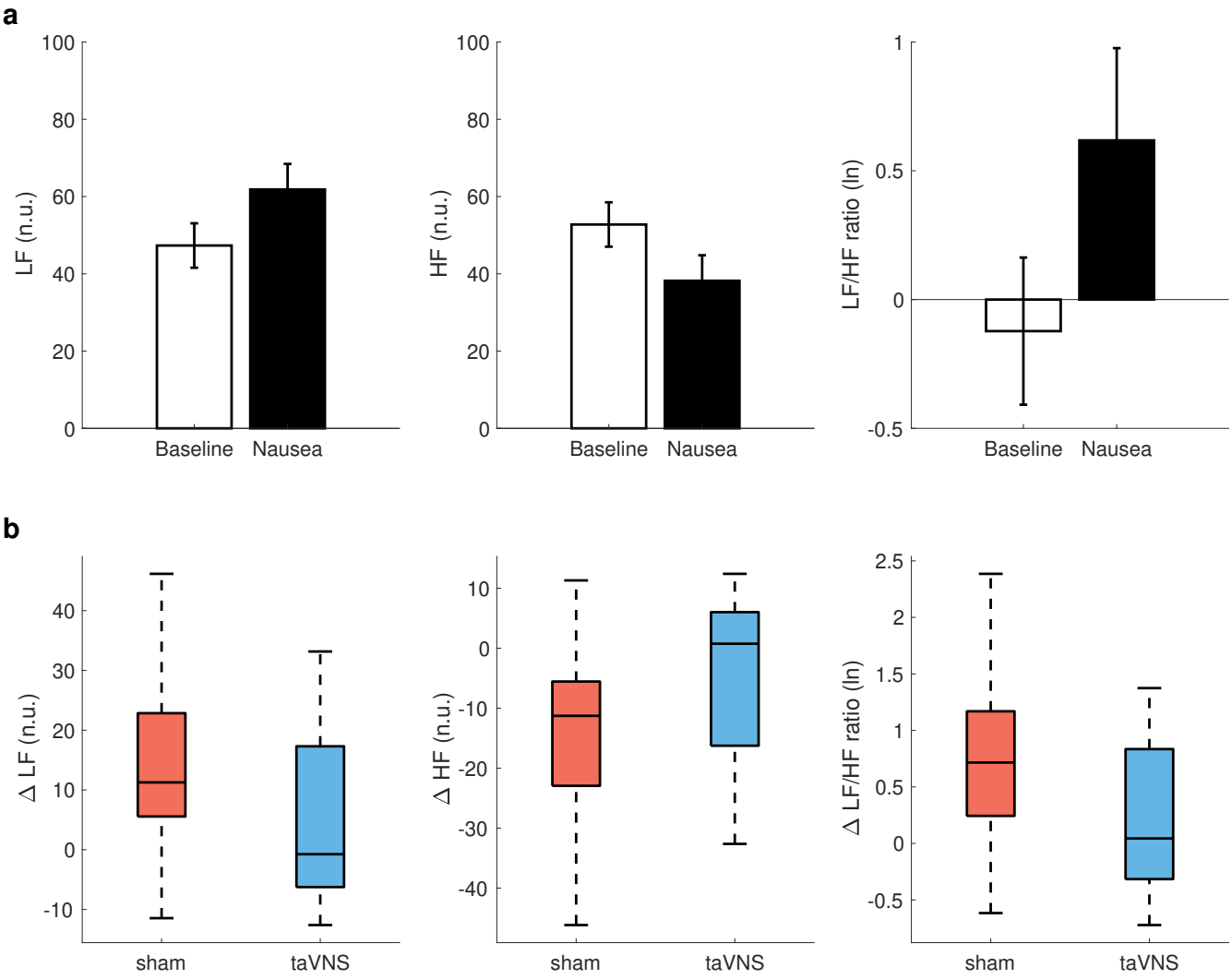

Figure 1. Spectral heart rate variability (HRV) measurements between participants at baseline and "Nausea" section, and between sham and transcutaneous auricular vagus nerve stimulation (taVNS) condition. **(a)** Average spectral power of low frequency (LF) and high frequency (HF), and LF/HF power ratio in response to nauseogenic stimuli. **(b)** Average change in LF, HF and LF/HF ratio in participants during sham and taVNS condition. Error bars represent standard error of the mean (SEM). The box plot central marks, box edges and whiskers represent medians, 25th to 75th percentiles and data range, respectively.

assess normality. Subsequently, statistical differences in the MSAQ data between sham and taVNS conditions were evaluated by a non-parametric Wilcoxon signed rank test. MSAQ total score was found to be significantly lower in the taVNS condition compared to the sham condition ($p = 0.0166$) (Fig. 3a). A significant decrease was found in the Central ($p = 0.0049$) and Sopite ($p = 0.0342$) category subscores during taVNS compared to sham. The decrease in sickness symptoms that is observed in (Fig. 3b) for the Gastrointestinal and Peripheral category subscores did not reach statistical significance between sham and taVNS conditions (Gastrointestinal: $p = 0.3125$; Peripheral: $p = 0.2188$).

Discussion

This study provides initial insights in the therapeutic potential of taVNS for reducing visually induced motion sickness. We demonstrate that the spectra and time-varying features of HRV differ significantly when comparing sham and taVNS conditions. Whereby taVNS increases parasympathetic cardiac modulation and reduces the activity of the sympathetic nerves, supporting our hypothesis. Moreover, we show that the total MSAQ scores and MSAQ categorical subscores for the central and sopite dimensions were significantly lower in the taVNS condition when compared to the sham condition.

Because motion sickness has been implicated with decreased parasympathetic activity, and in turn contributing to perturbed autonomic function, we asked if taVNS could trigger restoration of sympathovagal balance while potentiating vagal tone in

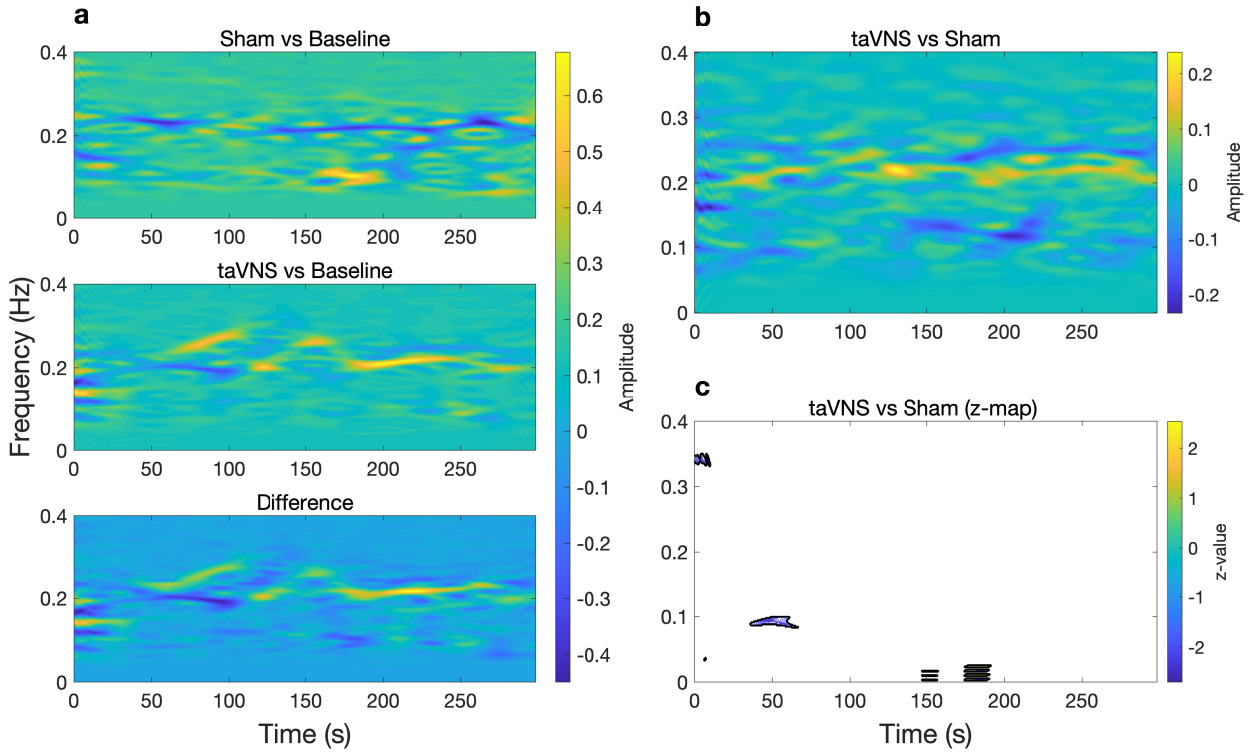

Figure 2. Time-varying power representations of heart rate variability (HRV) using the smoothed pseudo Wigner-Ville distribution (SPWVD). **(a)** Time-frequency power during sham (baseline subtracted) condition (top panel), taVNS (baseline subtracted) condition (middle panel) and difference between middle and top panels (bottom panel) in one example participant. **(b)** Time-frequency power representation at the sample level showing the power differences in taVNS and sham condition (after baseline subtraction within each condition). **(c)** Statistical z-map of the time-frequency power representation at the sample level, based on a cluster-level significance threshold $p < 0.05$ (two-sided non-parametric permutation tests). Significant clusters (regions) are indicated by black contours on the statistical z-map.

order to reduce symptoms. Although at the mechanistic level we still lack a clear understanding of how stimulating the vagus generates therapeutic effects[19,20], evidence from studies done both in animals[21,22] and humans[23,24] indicate that the seesaw of autonomic function can be altered by stimulating the vagus nerve. If we consider the vagus nerve to be a naturally available tool within our bodies to regulate calmness, then our rationale is that electrical stimulation may activate the parasympathetic nerves to lower the stress on the nervous system caused by the build up of factors inducing motion sickness.

Parasympathetic neural activity was significantly greater in taVNS conditions compared to sham as measured by HF power (Fig. 1b). This suggests that participants were symptomatic in the sham condition and asymptomatic in the taVNS condition on the basis that decreased parasympathetic modulation has been found during increasing levels of motion sickness. Importantly, it indicates that taVNS enhanced vagal tone in the physiology of the participants. Recent evidence corroborates our finding that taVNS improves HF power[24]. A possible explanation for this could be that our stimulation approach 'excites' the afferent fibers of the vagus nerve[25], thus sending a neural signal to the nucleus of the solitary tract (NTS) in the brainstem[26]. Exiting the brainstem, at the nucleus ambiguus and the dorsal motor nucleus of the vagus[25–27], are the efferent fibers of vagus nerve that carry parasympathetic innervation, leading to a measurable HF response.

Previous work showed that taVNS can reduce sympathetic nerve activity[23], and therefore, yield parasympathetic predominance. These observations align with the present study, and here we show that individuals exposed to nauseogenic stimuli causing an aversive experience, have reduced sympathetic nerve outflow during taVNS intervention. This suggests taVNS may be eliciting effects of less agitation and as such, positively influencing autonomic response toward a desirable state of well-being. Parasympathetic and sympathetic systems can be considered foils of each other. Therefore, the explanation for parasympathetic activation from above, would mean inhibition of efferent sympathetic activity may be the reason we found reduced LF power, and consequentially, reduced sympathovagal balance as measured by LF/HF ratio (Fig. 1b).

In addition to HRV static spectral analysis, we computed the time-frequency features of HRV using SPWVD. Despite

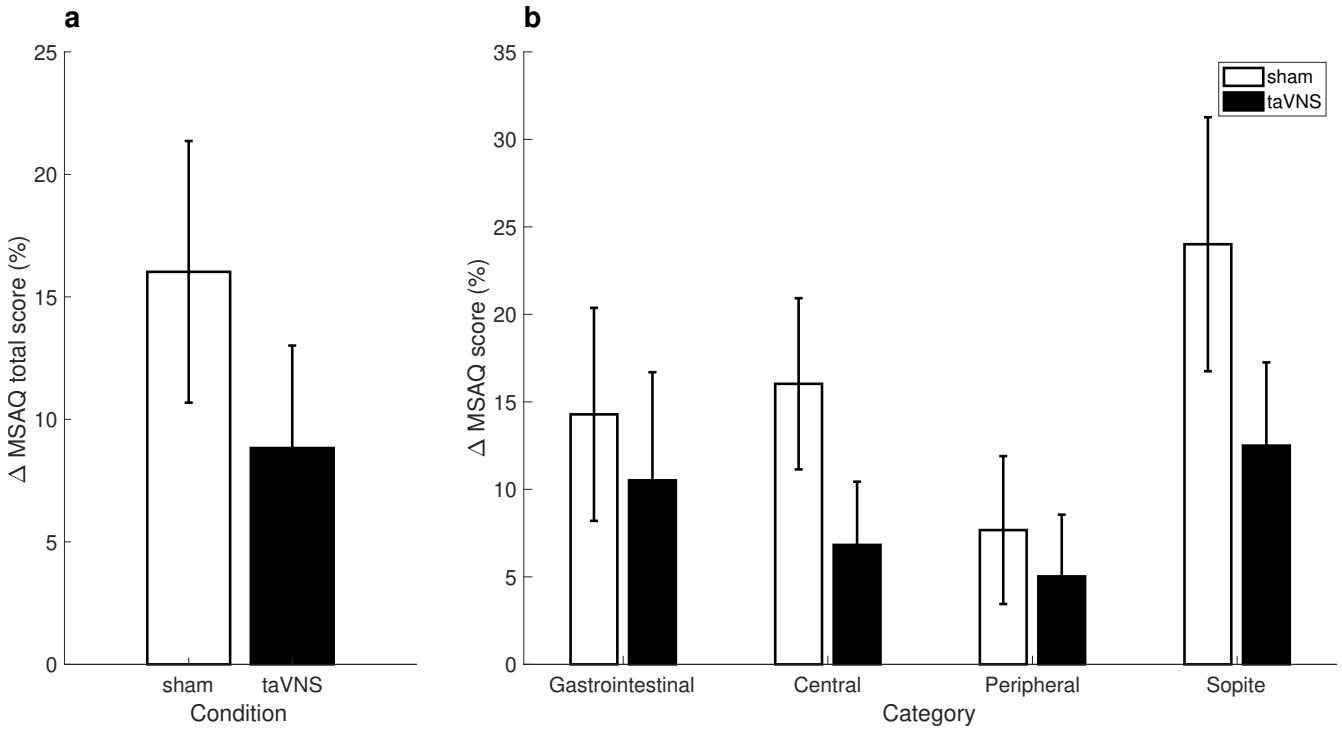

Figure 3. Summary of motion sickness assessment questionnaire (MSAQ) total and subscale scores across participants. **(a)** Average change in MSAQ total scores between sham and taVNS condition. **(b)** Average change in MSAQ scores within each category (gastrointestinal, central, peripheral, sopite) between sham and taVNS condition. Data are shown as mean ± SEM.

this being the first time, to the authors knowledge, that SPWVD is being applied in the context of motion sickness-associated ANS response; it may well allow us to discern the complexities of malaise progression. The time-varying power maps suggest motion sickness influences normal regulation of autonomic function by attenuating the activity of the HF component (Fig. 2a; Sham vs Baseline panel). Of note, this HF power attenuation appears to be portrayed by phasic alterations over time, perhaps simulating autonomic flushes that are implicated with cardiovagal bursts precursory nausea rating[15]. In Fig. 2a (taVNS vs Baseline panel), we observe the time-varying evolution of autonomic activity when taVNS is administered simultaneously with sickness-inducing stimuli. Interestingly, we observe that taVNS (Fig. 2a; Difference panel) is able to fairly restore autonomic imbalance that we saw in the untreated (sham) condition (Fig. 2a; Sham vs Baseline panel). In particular, it is now easy to see the frequency component around 0.25 Hz that is driven by respiratory modulation. This respiratory modulation tends to be disrupted in the sham condition suggesting that motion sickness enhances lower frequency components while concurrently reducing parasympathetic modulation; indicating an increased level of autonomic arousal. Taken together, the time-frequency maps presented in (Fig. 2) may be useful to distinguish malaise severity between sham and taVNS.

Our findings from the MSAQ data showed significant decreases in the total scores and in all but two categorical subscores (gastrointestinal and peripheral) between sham and taVNS condition. Although there were no significant differences found for the gastrointestinal and peripheral category subscores, decreases were present as can be observed in (Fig. 3b). One possible explanation for this result could be an underreporting of sickness symptoms in the sham condition due to a negative emotion experienced from the nauseogenic stimulus. This could be driven by the markedly decreased MSAQ scores in the sopite category where we can find individual symptoms of 'I felt annoyed/irritated', 'I felt drowsy', 'I felt tired/fatigued' and 'I felt uneasy'[28]. This dominance of sopite-like symptoms may have clouded participant judgement in reliably reporting how they felt after the experiment. Previous research has also suggested male participants may have a motion sickness response bias[29]. In addition, participants may have been cognitively constrained to reliably report their symptoms post-experiment as motion sickness is implicated with decreased cognitive performance[30]. Conceivably, the physiology of some participants may have been more responsive to the aversive experience of motion sickness and thus overshadowing the effects of taVNS. We have long known that susceptibility to the malaise of motion sickness is a highly individual experience[31]. Moreover, stimulation of the vagus nerve has individual variability in and of itself[32].

Our study is not without limitations. First, the sample size in our study was small. In addition, the study did not include a matching or sufficient number of male participants. Nevertheless, our findings suggest that motion sickness can be reduced by

transcutaneously stimulating the vagus nerve. Thus, suggesting important implications for establishing treatment interventions based on taVNS for motion sickness-related conditions. Participant cohort were naïve to the nauseogenic stimuli and taVNS stimulation. The stimulation parameters utilised in this study were well-tolerated by all participants and no unexpected adverse effects were reported. While some participants prematurely stopped the presentation of nauseogenic stimulus due to a high severe feeling of nausea, no one vomited at the end of stimulus presentation. Future research is warranted where the findings here are augmented by the assessment of physiological correlates of motion sickness (i.e., neuroendocrine hormones such as arginine vasopressin and norepinephrine[33]). Moreover, the key questions to look forward to include; could we identify optimal stimulation parameters to improve effects of taVNS toward motion sickness reduction, and could increased stimulation duration improve efficacy of taVNS to ameliorate motion sickness? In our future research, our investigations will extend to these questions and also administer an individually adjusted electrical current intensity.

In conclusion, insights from our data showed for the first time that taVNS stimulation elicits positive effects on reducing the symptoms of visually induced motion sickness. Our results potentially mark a significant step into preventing or slowing the onset of motion sickness, an incurable malady. With taVNS exhibiting notable efficacy, being able to study further and understand the mechanisms and pathways underlying its effects toward counter-motion sickness would enable us to deeply exploit its potential for optimum therapeutic outcomes. Further, tailoring taVNS stimulation to the individual participant, that is, precision treatment via taVNS, may perhaps be a much more effective strategy in an aim to non-pharmacologically mitigate motion sickness. Together, our findings suggest taVNS as a safe, reliable and effective tool with potentially important therapeutic implications for motion sickness.

Methods

Participants

Sixteen healthy participants were recruited for the study. Of the 16 participants, 14 were retained (mean age $\pm$ S.D. = 26.7 $\pm$ 4.0 years, age range = 21-34 years, 12 females) for further analysis after 2 were excluded due to unsaved data and loss of follow-up respectively. Participant cohort had normal or corrected-to-normal vision. Inclusion criteria were no medical history of stroke, epilepsy or any neurological disorders. Additionally, participants were not using cardiac pacemakers, had no metal plates and were not on any medication. Participants received financial compensation (£30) in the form of an Amazon gift voucher for their participation. The methods were approved by the Central Research Ethics Advisory Group (ref: CREAG015-12-2021) of the University of Kent. Prior to participation, written informed consent was obtained from all participants. All study methods conformed to the principles set by the Declaration of Helsinki.

Experimental protocol

The experimental paradigm was designed as a within-participants cross-over study where each participant visited the lab for sham and active taVNS sessions. To allow for a washout period, sessions for sham and active taVNS were on separate days, with a minimum of 1 week in between. The order in which sham and active taVNS were administered was randomly assigned. Participants completed a pre- and post-MSAQ during both sessions. During both sham and taVNS sessions, participants observed a black crosshair projected at the centre of a screen for 5 minutes (baseline), followed by the Nauseogenic stimulus for a maximum of 20 minutes, and finally, a further black crosshair for 5 minutes (recovery) projected similar to baseline (Fig. 4c). Simultaneous to the presentation of the nauseogenic stimulus, the electrode of the taVNS stimulator was clipped to the earlobe of the left ear for sham sessions (Fig. 4b) and for taVNS sessions, to the tragus of the left ear (Fig. 4a). At the subjective level of experiencing a severe sensation of nausea, the participant would stop the presentation of nauseogenic stimulus by pressing a button on a keypad. Participants also provided subjective ratings to report their level of nausea by pressing on a keypad where (0 = “no nausea”), (1 = “mild”), (2 = “moderate”) and (3 = “strong”). Regardless of whether the participant stopped the stimulus prematurely or the 20 minutes elapsed, the recovery section always followed. From the beginning of the baseline section through to the end of the recovery section, ECG measurements were being recorded continuously. The researcher was with the participant in the lab during data acquisition proceedings, both to ensure the safety of the participant and to monitor smooth running of the experiment. Of note, the researcher was not in the view of the participant during the stimulus presentation. Participants were instructed to focus on the stimulus throughout, minimise conversation and to avoid body movements during the data acquisition process.

Nauseogenic stimulus

We created a nauseogenic visual stimulus to induce nausea. MATLAB (The MathWorks, Inc., Natick, MA, USA) software was used to develop source code for the nauseogenic visual stimulus using the Psychophysics Toolbox Version 3 (https://github.com/Psychtoolbox-3/Psychtoolbox-3)[34–36]. The stimulus was a horizontal translation of black and white vertical stripes with a circular shift of 62.5°/s (Fig. 4c). This computerised stimulus simulates the visual input provided by the classic rotating optokinetic drum utilised to induce motion sickness/nausea[37–39]. It is well-known in the literature that this translation

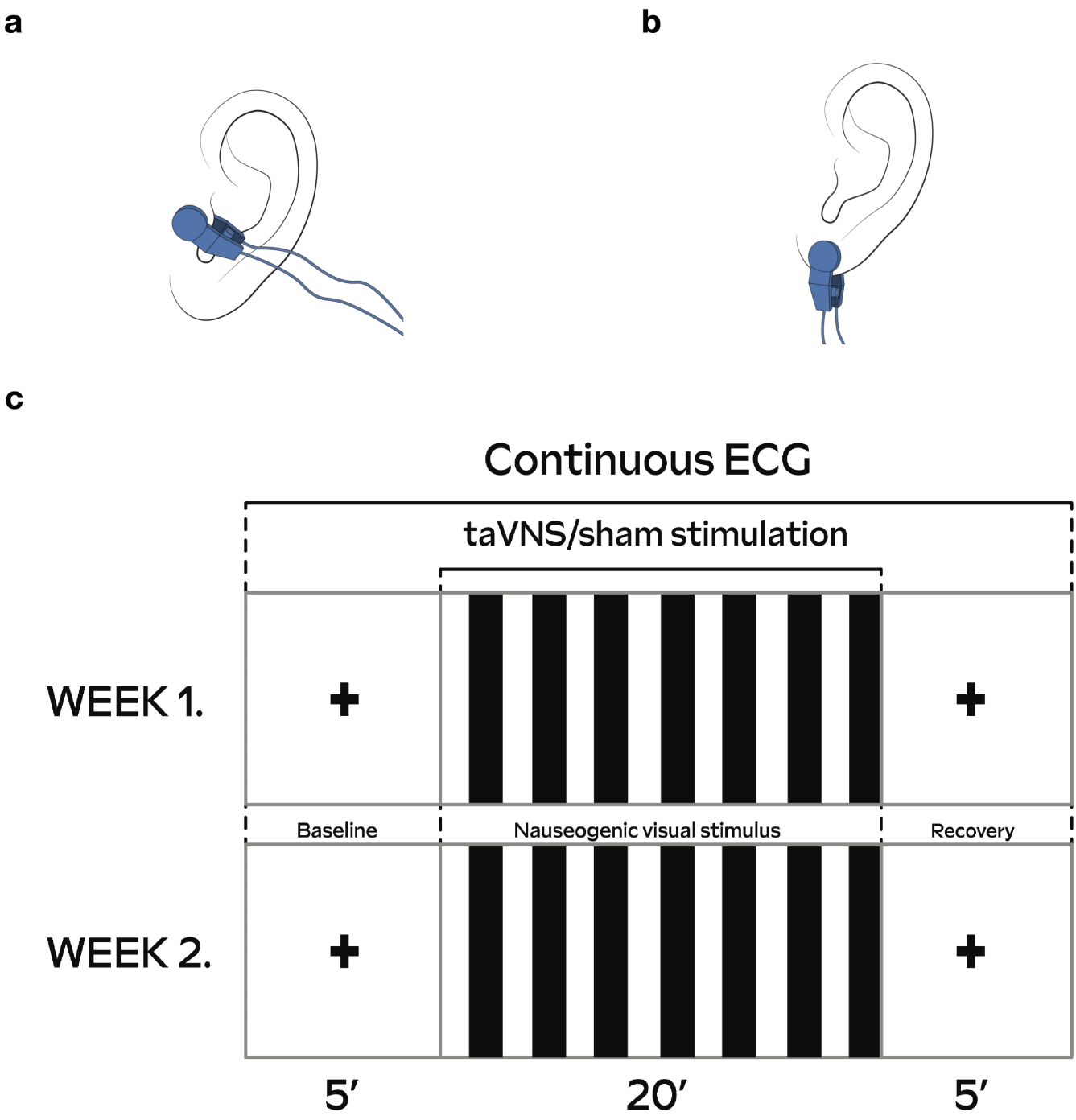

Figure 4. Experimental overview illustrations. **(a)** The electrode was clipped at the tragus site of the left ear during taVNS condition. **(b)** And clipped to the earlobe of the left ear during sham condition. **(c)** Participants underwent a baseline, nauseogenic visual stimulation and recovery section, respectively in both week 1 (first visit) and week 2 (follow-up visit), separated by 1 week. Electrocardiogram (ECG) signals were recorded continuously from beginning of baseline to end of recovery. Participants were randomly assigned to receive taVNS or sham in week 1 (first visit) and to receive opposite treatment on follow-up.

of alternating black and white stripes elicits illusory self-motion (vection) and nausea[40,41]. An fMRI compatible variant of the stimulus has been used effectively for inducing nausea in cardiac modulation and neuroimaging studies investigating motion sickness[14,15,42–45]. We presented the stimulus on a 47-inch LG LCD Widescreen (47LW450U, LG Electronics UK, UK) at a distance filling the participant's full visual field. The display refresh rate was 60 Hz. The complete and contiguous study

stimulus was a crosshair fixation section at baseline, nauseogenic stimulus section and a crosshair fixation section at recovery.

Electrical stimulation

Non-invasive taVNS was applied using the EM6300A TENS (Med-Fit UK Ltd, Stockport, UK) device; a battery driven medical vagus nerve stimulator with electrodes that can be clipped onto the ear (tragus or earlobe for example). Active taVNS was administered at the tragus site of the left ear (Fig. 4a); and sham administered to the left earlobe (Fig. 4b). Stimulation current was delivered as asymmetric biphasic square-wave pulses with a pulse width of 200 μs, pulse frequency of 20 Hz and current intensity of 1.0 mA. Stimulation parameters were chosen based on literature assessing autonomic modulation. The parameters were tested prior to beginning each experimental session. The stimulation device was triggered manually by the researcher and had a countdown timer set for 20 minutes, in synchrony with the maximum duration of the nauseogenic stimulus. Moreover, the researcher turned off the device when the 20 minutes elapsed. In addition, the researcher immediately turned off the device for scenarios involving participants stopping the nauseogenic stimulus prematurely. Perception of the above-mentioned stimulation parameters was reported by all participants without painful sensation.

ECG data acquisition, processing and analysis

Continuous ECG data acquisition was performed using a BioSemi ActiveTwo system (BioSemi B, V., Amsterdam, Netherlands). During the experiment, 64-channel electroencephalography (EEG) activity was also recorded. EEG data will be presented in a separate publication, allowing scope for discussion focused on ANS response for current analysis. The ECG signal was digitized at a sampling rate of 256 Hz using LabVIEW (National Instruments, USA) software. Electrode signal transduction was optimised by applying SIGNAGEL conductive gel. Electrode offset was within $\pm$ 10 μV. The recorded data was persisted as .bdf files for offline processing. ECG signal processing and analysis was performed using custom code developed in MATLAB software in accordance with recommended standards for HRV signals[46]. First, raw ECG data was visually inspected for any disturbances or distortions. Epochs of 5 minutes were extracted from the continuous ECG data for 'Baseline' and 'Nausea' sections. The logic for extracting epochs of the 'Nausea' section was as follows: if the participant completed the whole 20-minute section without a subjective rating of at least 2 (moderate nausea), then the 5-minute epoch was obtained from right before the recovery section started. If the participant had a subjective rating of at least 2, then the 5-minute epoch was obtained from right before the maximum rating was triggered. For scenarios where the participant prematurely stopped the nauseogenic stimulation due to a subjective severe feeling of nausea rating, then the 5-minute epoch was obtained from right before the recovery section followed (note that the recovery section followed regardless of natural or subjective stoppage of the nauseogenic stimulation). Using the obtained 5-minute ECG epochs, we performed R-peak detection using the Pan-Tompkins algorithm[47] and subsequently, the RR time-series (RR intervals) were generated. The *filtfilt* MATLAB function was used for implementation of ECG waveform filters in order to perform zero-phase digital filtering. Visual inspection was performed to ensure the quality of the RR series retained.

Frequency domain analysis

To perform spectral analysis of the HRV, we first detrended the obtained RR series using the smoothness priors method[48]. We used a value of 100 for the parameter *lambda* for smoothness priors detrending. Essentially, this method operates similarly to a time-varying finite impulse response (FIR) high pass filter, in order to address the nonstationarity problem in the HRV signal. The Lomb-Scargle periodogram was then used to perform power spectral density (PSD) estimation on the detrended signal. Subsequently, we computed the total power of HRV spectra (Total power; $\leq$ 0.40 Hz), and the power of very low frequency (VLF; $\leq$ 0.04 Hz), low frequency (LF; 0.04-0.15 Hz), high frequency (HF; 0.15-0.40 Hz) and the power ratio of LF to HF (LF/HF). Note that VLF power was only calculated to compute LF and HF in normalized units (n.u.) using formulae below[46], and we took the natural logarithm (ln) of the LF/HF ratio.

$$LF_{norm} = \frac{LF\ power}{Total\ power - VLF\ power} \times 100 \tag{1}$$

$$HF_{norm} = \frac{HF\ power}{Total\ power - VLF\ power} \times 100 \tag{2}$$

$$lnLF/HF_{ratio} = \log\left(\frac{LF\ power}{HF\ power}\right) \tag{3}$$

Time-Frequency representation analysis

We sought to perform time-frequency analysis knowing that this has the added advantage of observing how the frequency components of a signal varies over time. Thus, being able to observe the progression of symptoms as the participant suffers bouts of sickness may help elucidate how motion sickness evolves, in addition to how taVNS may be involved in the sickness evolution process. First, we applied cubic spline interpolation to the RR series obtained; with simultaneous resampling at 4 Hz. Then RR detrending was performed as previously described (see Frequency domain analysis). The Hilbert transform was applied to obtain the analytic signal association to the HRV signal. Then we performed smoothed pseudo Wigner-Ville distribution (SPWVD) to compute time-frequency power. The SPWVD is a well-known method for its good time-frequency resolution and robustness towards cardiovascular signal analysis[49]. Previous studies have utilised the SPWVD method to detect obstructive sleep apnea (OSA) in ECG recordings (e.g.[50]) in addition to drowsiness detection (e.g.[51]). The SPWVD is a member of the Cohen's class family of time-frequency distributions[52], and can be defined as follows:

$$SPWVD_x^{g,H}(t,f) = \int_{-\infty}^{\infty} g(t)\,H(f)\,x\left(t+\frac{\tau}{2}\right)x^*\left(t-\frac{\tau}{2}\right)e^{-j2\pi ft}d\tau \tag{4}$$

The term $g(t)$ represents performing a convolution (smoothing) in time. Whereas, the term $H(f)$ represents spectral smoothing of $g(t)$ using a nonparametric fast Fourier transformation (FFT). Of utmost importance, by looking at the local features of the signal x in time t, SPWVD enables independent smoothing in time and in frequency[53].

Motion sickness questionnaire

In order to assess symptoms of motion sickness, participants completed the motion sickness assessment questionnaire (MSAQ)[28] before and after the experiment. The MSAQ is a well-known validated tool consisting of 16 symptoms categorised into 4 dimensions of motion sickness defined as gastrointestinal, central, peripheral and sopite-related. The individual symptoms are rated on a nine-point scale where (1 = "not at all") and (9 = "severely"). The MSAQ total score is computed as a percentage of summed points from all symptoms. While scores for the 4 categories are percentages of summed points from within each category.

Statistical analysis

All statistical analyses were performed using MATLAB software. We reported variables of the HRV spectra and the MSAQ as means with standard error (SEM). Changes of HRV spectral data were analysed using a paired t-test. We used non-parametric cluster-based permutation tests[54] to examine the differences in the time-frequency representations of SPWVD at the sample level between sham and taVNS condition. Herein, it is important to note the necessity of cluster-based permutation tests on time-frequency data. From the basis of a significance threshold at ($p = 0.05$), we computed a z-value, which, in turn, was used to threshold the z-transformed time-frequency power difference between taVNS and sham condition. To generate a null distribution, we performed 1000 random permutations, where at each permutation extracting the maximum cluster mean of the z-values. Our analysis is based on discussing the temporal clusters found as shown in (Fig. 2c). However, it is worthy of caution that clusters identified using this method may represent effects detected though maybe not supported by the permutation test[55]. The changes in the MSAQ were assessed for normality using the Shapiro-Wilk test[56] and subsequently analysed using a non-parametric Wilcoxon signed rank test. Statistical significance was considered at ($p < 0.05$).

Data availability

The datasets generated and analysed during the current study and the analysis code are available from the corresponding author upon reasonable request.

References

1. Stefan, H. *et al.* Transcutaneous vagus nerve stimulation (t-VNS) in pharmacoresistant epilepsies: A proof of concept trial. *Epilepsia* **53**, e115–e118, DOI: https://doi.org/10.1111/j.1528-1167.2012.03492.x (2012).
2. Hein, E. *et al.* Auricular transcutaneous electrical nerve stimulation in depressed patients: a randomized controlled pilot study. *J. Neural Transm.* **120**, 821–827, DOI: 10.1007/s00702-012-0908-6 (2013).
3. Straube, A., Ellrich, J., Eren, O., Blum, B. & Ruscheweyh, R. Treatment of chronic migraine with transcutaneous stimulation of the auricular branch of the vagal nerve (auricular t-VNS): a randomized, monocentric clinical trial. *The J. Headache Pain* **16**, 63, DOI: 10.1186/s10194-015-0543-3 (2015).
4. Mondal, B. *et al.* Non-invasive vagus nerve stimulation improves clinical and molecular biomarkers of Parkinson's disease in patients with freezing of gait. *npj Park. Dis.* **7**, 46, DOI: 10.1038/s41531-021-00190-x (2021).

5. Yuan, H. & Silberstein, S. D. Vagus Nerve and Vagus Nerve Stimulation, a Comprehensive Review: Part I. *Headache: The J. Head Face Pain* **56**, 71–78, DOI: https://doi.org/10.1111/head.12647 (2016).

6. Reason, J. & Brand, J. *Motion Sickness* (Academic Press, 1975).

7. Kuiper, O. X., Bos, J. E. & Diels, C. Looking forward: In-vehicle auxiliary display positioning affects carsickness. *Appl. Ergonomics* **68**, 169–175, DOI: https://doi.org/10.1016/j.apergo.2017.11.002 (2018).

8. Lackner, J. R. Motion sickness: Our evolving understanding and problems. In *Reference Module in Neuroscience and Biobehavioral Psychology*, DOI: https://doi.org/10.1016/B978-0-12-809324-5.21621-0 (Elsevier, 2019).

9. Merhi, O., Faugloire, E., Flanagan, M. & Stoffregen, T. A. Motion sickness, console video games, and head-mounted displays. *Hum. Factors* **49**, 920–934, DOI: 10.1518/001872007X230262 (2007). PMID: 17915607.

10. Keshavarz, B. & Hecht, H. Stereoscopic viewing enhances visually induced motion sickness but sound does not. *Presence* **21**, 213–228, DOI: 10.1162/PRES_a_00102 (2012).

11. Reason J. Motion sickness adaptation: a neural mismatch model! *J. Royal Soc. Medicine* **71**, 819–829 (1978).

12. Gianaros, P. J. *et al.* Relationship between temporal changes in cardiac parasympathetic activity and motion sickness severity. *Psychophysiology* **40**, 39–44, DOI: https://doi.org/10.1111/1469-8986.00005 (2003).

13. Yokota, Y., Aoki, M., Mizuta, K., Ito, Y. & Isu, N. Motion sickness susceptibility associated with visually induced postural instability and cardiac autonomic responses in healthy subjects. *Acta Oto-Laryngologica* **125**, 280–285, DOI: 10.1080/00016480510003192 (2005).

14. Kim, J., Napadow, V., Kuo, B. & Barbieri, R. A combined HRV-fMRI approach to assess cortical control of cardiovagal modulation by motion sickness. In *2011 Annual International Conference of the IEEE Engineering in Medicine and Biology Society*, 2825–2828 (IEEE, 2011).

15. LaCount, L. T. *et al.* Static and dynamic autonomic response with increasing nausea perception. *Aviat. space, environmental medicine* **82**, 424–433 (2011).

16. Lin, C.-T., Lin, C.-L., Chiu, T.-W., Duann, J.-R. & Jung, T.-P. Effect of respiratory modulation on relationship between heart rate variability and motion sickness. In *2011 Annual International Conference of the IEEE engineering in medicine and biology society*, 1921–1924 (IEEE, 2011).

17. Sawada, Y. *et al.* Effects of synchronised engine sound and vibration presentation on visually induced motion sickness. *Sci. Reports* **10**, 7553, DOI: 10.1038/s41598-020-64302-y (2020).

18. Zhao, Q. *et al.* Transcutaneous Electrical Acustimulation Ameliorates Motion Sickness Induced by Rotary Chair in Healthy Subjects: A Prospective Randomized Crossover Study. *Neuromodulation* DOI: 10.1016/j.neurom.2021.09.004 (2022).

19. Vonck, K. E. & Larsen, L. E. Chapter 18 - vagus nerve stimulation: Mechanism of action. In Krames, E. S., Peckham, P. H. & Rezai, A. R. (eds.) *Neuromodulation (Second Edition)*, 211–220, DOI: https://doi.org/10.1016/B978-0-12-805353-9.00018-8 (Academic Press, 2018), second edition edn.

20. Johnson, R. L. & Wilson, C. G. A review of vagus nerve stimulation as a therapeutic intervention. *J. inflammation research* **11**, 203 (2018).

21. Iwao, T. *et al.* Effect of constant and intermittent vagal stimulation on the heart rate and heart rate variability in rabbits. *The Jpn. J. Physiol.* **50**, 33–39, DOI: 10.2170/jjphysiol.50.33 (2000).

22. Ardell, J. L., Rajendran, P. S., Nier, H. A., KenKnight, B. H. & Armour, J. A. Central-peripheral neural network interactions evoked by vagus nerve stimulation: functional consequences on control of cardiac function. *Am. J. Physiol. Circ. Physiol.* **309**, H1740–H1752, DOI: 10.1152/ajpheart.00557.2015 (2015). PMID: 26371171.

23. Clancy, J. A. *et al.* Non-invasive Vagus Nerve Stimulation in Healthy Humans Reduces Sympathetic Nerve Activity. *Brain Stimul. Basic, Transl. Clin. Res. Neuromodulation* **7**, 871–877, DOI: 10.1016/j.brs.2014.07.031 (2014).

24. Geng, D., Liu, X., Wang, Y. & Wang, J. The effect of transcutaneous auricular vagus nerve stimulation on HRV in healthy young people. *PLOS ONE* **17**, 1–17, DOI: 10.1371/journal.pone.0263833 (2022).

25. Murray, A. R., Atkinson, L., Mahadi, M. K., Deuchars, S. A. & Deuchars, J. The strange case of the ear and the heart: The auricular vagus nerve and its influence on cardiac control. *Auton. Neurosci. Basic Clin.* **199**, 48–53, DOI: 10.1016/j.autneu.2016.06.004 (2016).

26. Kaniusas, E. *et al.* Current Directions in the Auricular Vagus Nerve Stimulation I – A Physiological Perspective. *Front. Neurosci.* **13**, DOI: 10.3389/fnins.2019.00854 (2019).

27. Ellrich, J. Transcutaneous Auricular Vagus Nerve Stimulation. *J. Clin. Neurophysiol.* **36** (2019).

28. Gianaros, P. J., Muth, E. R., Mordkoff, J. T., Levine, M. E. & Stern, R. M. A questionnaire for the assessment of the multiple dimensions of motion sickness. *Aviat. space, environmental medicine* **72**, 115 (2001).

29. Fessler, D. M. & Arguello, A. P. The relationship between susceptibility to nausea and vomiting and the possession of conditioned food aversions. *Appetite* **43**, 331–334, DOI: https://doi.org/10.1016/j.appet.2004.10.001 (2004).

30. Park, S., Kim, L., Kwon, J., Choi, S. J. & Whang, M. Evaluation of visual-induced motion sickness from head-mounted display using heartbeat evoked potential: a cognitive load-focused approach. *Virtual Real.* DOI: 10.1007/s10055-021-00600-8 (2021).

31. Reason, J. Individual differences in motion sickness susceptibility: A further test of the 'receptivity' hypothesis. *Br. J. Psychol.* **60**, 321–328 (1969).

32. Schuerman, W. L. *et al.* Human intracranial recordings reveal distinct cortical activity patterns during invasive and non-invasive vagus nerve stimulation. *Sci. Reports* **11**, 22780, DOI: 10.1038/s41598-021-02307-x (2021).

33. Otto, B., Riepl, R. L., Klosterhalfen, S. & Enck, P. Endocrine correlates of acute nausea and vomiting. *Auton. Neurosci. Basic Clin.* **129**, 17–21, DOI: 10.1016/j.autneu.2006.07.010 (2006).

34. Brainard, D. H. The Psychophysics Toolbox. *Spatial vision* **10 4**, 433–6 (1997).

35. Pelli, D. The VideoToolbox software for visual psychophysics: transforming numbers into movies. *Spatial vision* **10 4**, 437–42 (1997).

36. Kleiner, M., Brainard, D. H. & Pelli, D. What's new in Psychtoolbox-3? *Perception* **36**, 1–16 (2007).

37. Stern, R. *et al.* Tachygastria and motion sickness. *Aviat. space, environmental medicine* **56**, 1074–1077 (1985).

38. Bos, J. E. & Bles, W. Motion sickness induced by optokinetic drums. *Aviat. space, environmental medicine* **75**, 172–174 (2004).

39. Levine, M. E., Stern, R. M. & Koch, K. L. Enhanced perceptions of control and predictability reduce motion-induced nausea and gastric dysrhythmia. *Exp. Brain Res.* **232**, 2675–2684, DOI: 10.1007/s00221-014-3950-9 (2014).

40. Koch, K. Illusory self-motion and motion sickness: a model for brain-gut interactions and nausea. *Dig. diseases sciences* **44**, 53S–57S (1999).

41. Kennedy, R. S., Drexler, J. & Kennedy, R. C. Research in visually induced motion sickness. *Appl. Ergonomics* **41**, 494–503, DOI: https://doi.org/10.1016/j.apergo.2009.11.006 (2010). Special Section - The First International Symposium on Visually Induced Motion Sickness, Fatigue, and Photosensitive Epileptic Seizures (VIMS2007).

42. Lacount, L. *et al.* Dynamic Cardiovagal Response to Motion Sickness: A Point-Process Heart Rate Variability Study. *Comput. cardiology* **36**, 49–52 (2009).

43. Napadow, V. *et al.* The brain circuitry underlying the temporal evolution of nausea in humans. *Cereb. cortex* **23**, 806–813 (2013).

44. Sclocco, R. *et al.* Brain circuitry supporting multi-organ autonomic outflow in response to nausea. *Cereb. cortex* **26**, 485–497 (2016).

45. Toschi, N. *et al.* Motion sickness increases functional connectivity between visual motion and nausea-associated brain regions. *Auton. Neurosci.* **202**, 108–113 (2017).

46. Task Force of the European Society of Cardiology and the North American Society of Pacing and Electrophysiology. Heart rate variability: Standards of measurement, physiological interpretation, and clinical use. *Circulation* **93**, 1043–1065, DOI: 10.1161/01.CIR.93.5.1043 (1996).

47. Pan, J. & Tompkins, W. J. A Real-Time QRS Detection Algorithm. *IEEE Transactions on Biomed. Eng.* **BME-32**, 230–236, DOI: 10.1109/TBME.1985.325532 (1985).

48. Tarvainen, M., Ranta-aho, P. & Karjalainen, P. An advanced detrending method with application to HRV analysis. *IEEE Transactions on Biomed. Eng.* **49**, 172–175, DOI: 10.1109/10.979357 (2002).

49. Orini, M., Bailon, R., Mainardi, L. T., Laguna, P. & Flandrin, P. Characterization of dynamic interactions between cardiovascular signals by time-frequency coherence. *IEEE Transactions on Biomed. Eng.* **59**, 663–673, DOI: 10.1109/TBME.2011.2171959 (2012).

50. Quiceno-Manrique, A. F., Alonso-Hernandez, J. B., Travieso-Gonzalez, C., Ferrer-Ballester, M. A. & Castellanos-Dominguez, G. Detection of obstructive sleep apnea in ECG recordings using time-frequency distributions and dynamic features. In *2009 Annual International Conference of the IEEE Engineering in Medicine and Biology Society*, 5559–5562, DOI: 10.1109/IEMBS.2009.5333736 (2009).

51. Vicente, J., Laguna, P., Bartra, A. & Bailón, R. Drowsiness detection using heart rate variability. *Med. & Biol. Eng. & Comput.* **54**, 927–937, DOI: 10.1007/s11517-015-1448-7 (2016).

52. Cohen, L. *Time-frequency analysis*, vol. 778 (Prentice hall New Jersey, 1995).

53. Pola, S., Macerata, A., Emdin, M. & Marchesi, C. Estimation of the power spectral density in nonstationary cardiovascular time series: assessing the role of the time-frequency representations (TFR). *IEEE Transactions on Biomed. Eng.* **43**, 46–, DOI: 10.1109/10.477700 (1996).

54. Maris, E. & Oostenveld, R. Nonparametric statistical testing of EEG-and MEG-data. *J. neuroscience methods* **164**, 177–190 (2007).

55. Sassenhagen, J. & Draschkow, D. Cluster-based permutation tests of MEG/EEG data do not establish significance of effect latency or location. *Psychophysiology* **56**, e13335, DOI: https://doi.org/10.1111/psyp.13335 (2019).

56. Shapiro, S. S. & Wilk, M. B. An analysis of variance test for normality (complete samples). *Biometrika* **52**, 591–611 (1965).

Acknowledgements

E.M. was supported by an Engineering and Physical Sciences Research Council PhD studentship at the University of Kent School of Computing (EP/T518141/1).

Author contributions

E.M. designed the experimental paradigm, did data collection, data analysis and drafted the manuscript. R.P. and I.M. conceptualised the idea and supervised E.M. in the project. All authors contributed to the manuscript writing and approved the final version of the manuscript.

Competing interests

The authors declare no competing interests.